RESEARCH ARTICLE

INTERNATIONAL RESEARCH JOURNAL OF MULTIDISCIPLINARY TECHNOVATION

Asian Research Association

DOI: 10.54392/irjmt2245

Mitigation of Starting Transients in Slip-Energy Recovery Drives

Sanaa M I Amer [1,*], Mona N Eskander [1]

[1] Power Electronics & Energy Conversion Department, Electronics Research Institute {ERI}, Joseph Tito St., Nozha, Cairo, Egypt.
* Corresponding author email: sanaa@eri.sci.eg
DOI: https://doi.org/10.54392/irjmt2245
Received: 25-05-2022; Revised: 21-07-2022; Accepted: 26-07-2022; Published: 30-07-2022

Abstract: Starting voltage and current transients in slip energy recovery drives (SERD) may damage the stator and rotor windings. The resulting torque oscillations damage the induction machine mechanical parts. In this paper three schemes for damping starting transients and torque oscillations are proposed. In the first scheme a parallel RL impedance is connected between the supply and the stator coils, in the second scheme a parallel RL impedance is added in the rotor circuit, and in the third scheme the two impedances are connected simultaneously. Transient performance is simulated and the results of the three schemes are compared. Also, the effect of each proposed scheme on the steady state values of the SERD currents, voltages, and electric torque is studied and demonstrated. Lower current and voltage transients, and lower torque oscillations resulted in all schemes, with optimum transient performance observed when adding the two impedances simultaneously.

Keywords: Slip Energy Recovery Drives (SERD), Transient Performance, Stator Impedance, Rotor Impedance

1. Introduction

The slip energy recovery drive, SERD, is a variable speed drive composed of a wound rotor induction motor whose rotor is connected to the grid via a diode rectifier, an inverter and a transformer. The speed control of the drive is achieved by regulating the rotor voltage by varying the on-off time of the inverter switches. It is characterized by its high efficiency due to transferring the wasted rotor power to the ac supply. Also, the lower rating of the rotor-converters results in lower drive cost. The SERD are widely used in industrial applications such as pumps, fans, and shipboard variable speed/constant frequency systems [1-6]. Variable starting methods are presented in the literature [7-12], such as direct line starting, variable frequency starting, reduced voltage starting by the use of solid-state switches, and soft starting. The cheapest starting method, that of direct line starting, causes high inrush currents, as well as current oscillations leading to torque oscillations. These may damage the motor windings and adversely affects the mechanical parts of the machine. Recent researches [13-15] proposed adding a parallel RC circuit in the stator circuit at starting and until reaching the steady state. However, the added capacitor, if not accurately designed, may lead to spikes due to charging and discharging cycles. Others proposed superconductor current limiter [15, 16], which is costly. The temperature rises due to starting transients is discussed in [17]. The effect of starting transients on distribution networks is studied in [18]. Control techniques for mitigation of motor starting voltage were proposed in [19, 20]. Protection method was studied in [21]. Starting Transient effects on loads was studied in [22].

In this paper direct starting is proposed with three proposed schemes; namely, adding an RL impedance between the ac supply and the stator, adding a RL impedance between the rotor circuit and the connected rectifier, and in the third scheme the two impedances are connected simultaneously. The results of the three cases are compared to conclude the optimum method for reducing the starting transients and torque oscillations. Also, the effect of each proposed scheme on the steady state values of the SERD currents, voltages, and electric torque is studied and demonstrated. Lower current and voltage transients, and lower torque oscillations resulted in all schemes, with optimum performance observed when adding the two impedances simultaneously. Although the steady state performance proved that adding the two impedances simultaneously led to decrease of rotor power delivered to the grid which decreases the efficiency of the SERD, however the voltage and current values of the steady state of the SERD are kept with rated values.

2. SERD Model

The machine dynamical equations in the d-q axis can be written as:

$$\frac{d\lambda_{ds}}{dt} = v_{ds} - r_s\, i_{ds} + W\lambda_{qs} \quad (1)$$

$$\frac{d\lambda_{qs}}{dt} = v_{qs} - r_s\, i_{qs} + W\lambda_{ds} \quad (2)$$

$$\frac{d\lambda_d}{dt} = v_{dr} - r_r\, i_{dr} + (W - W_r)\lambda_{dr} \quad (3)$$

$$\frac{d\lambda_{qr}}{dt} = v_{qr} - r_r\, i_{qr} - (W - W_r)\lambda_{dr} \quad (4)$$

$$\frac{d\omega_r}{dt} = \frac{1}{2H}(T_e - T_L - B_m W_r) \quad (5)$$

$$\lambda_{ds} = L_s i_{ds} + L_m i_{dr} \quad (6)$$

$$\lambda_{qs} = L_s i_{qs} + L_m i_{qr} \quad (7)$$

$$\lambda_{dr} = L_r i_{dr} + L_m i_{ds} \quad (8)$$

$$\lambda_{qr} = L_r i_{qr} + L_m i_{qs} \quad (9)$$

$$T_e = \frac{3PLm}{3L_s}(\lambda_{qs}\, i_{qr} - \lambda_{ds} i_{qr}) \quad (10)$$

Where …λ, v, i, ω, Te denote flux, voltage, current, angular speed and electromagnetic torque respectively. Subscripts d and q denote d-axis component and q-axis component in arbitrary d-q reference frame, respectively. r and L denote resistance and inductance, respectively. Suffixes s, r and m denote stator, rotor and mutual quantities respectively; P is the number of pole pairs

Figure 1 shows the configuration of the SERD. The SERD voltage and current equations in the d-q synchronously rotating frame are given as:

A PI controller is employed to regulate the speed of the drive to follow a reference speed. The drive model is simulated using Matlab/Simulink software. The voltages, currents, and electric torque of the drive with direct starting without a protection scheme are shown in figures 2-6, with steady state values imposed on each figure. The simulation results are presented at a reference speed equals 1.05 of the synchronous speed.

Figure. 2 show the stator voltage and current. The magnitude of the starting current is about ten times its steady state value, whose rms value is ± 5 amp.

The rotor voltage and current depicted in Figure. 3 shows extremely high transients for both voltage and current. The transient rotor voltage is about 20 times its steady state value, which is ± 45V, while the rotor transient current is about 25 times its steady state value, which is ± 2 amp.

Consequently, the stator and rotor active and reactive power, depicted on Figure 4 show sharp and high magnitudes at starting, which may damage the rectifier and inverter switches. The magnitude of the DC voltage peak at starting, reaches 1.4 times its steady state value (35V), while the magnitude of the DC current peak at starting is about 25 times its steady state value (2amp), as shown in Figure 5.

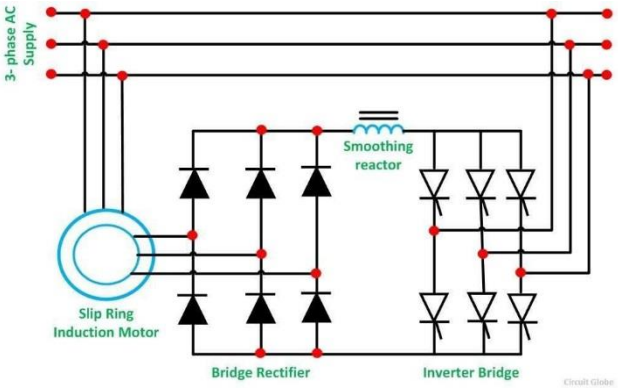

Figure 1. Basic Slip Energy Recovery Drive scheme

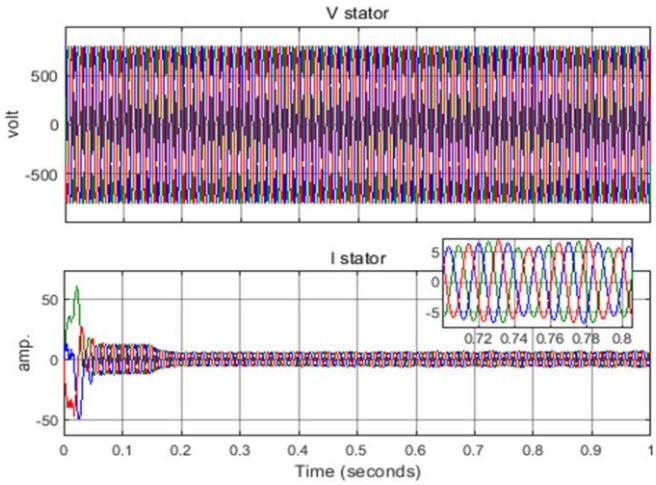

Figure 2. Stator voltage and current for direct starting of SERD

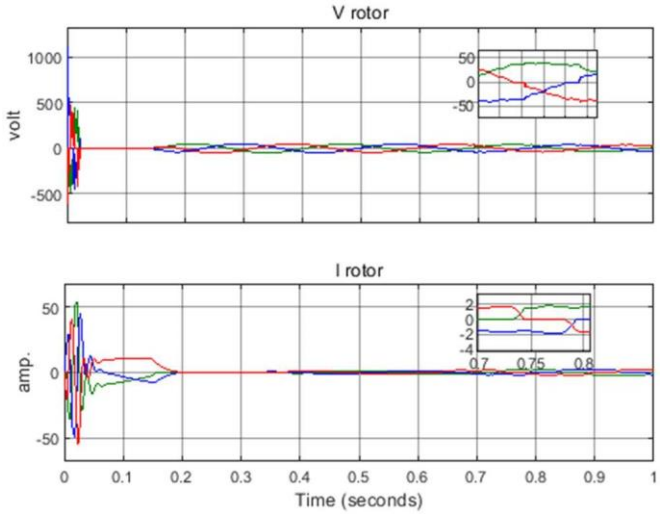

Figure 3. Rotor voltage and current with direct starting

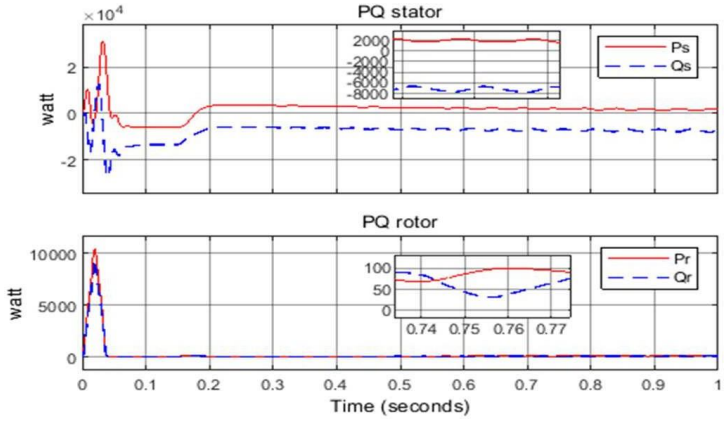

Figure 4. Active and reactive stator and rotor power with direct starting of SERD

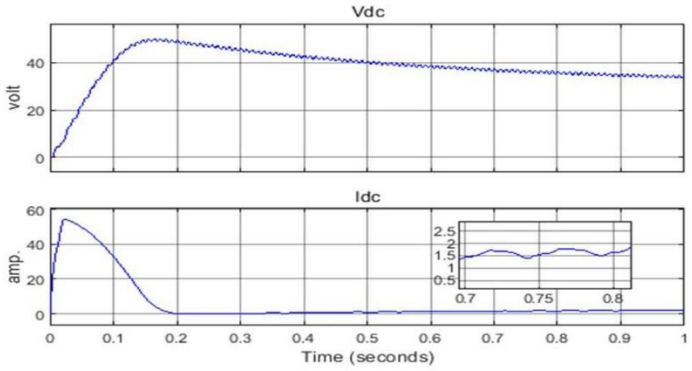

Figure 5. DC voltage and current at direct starting of SERD

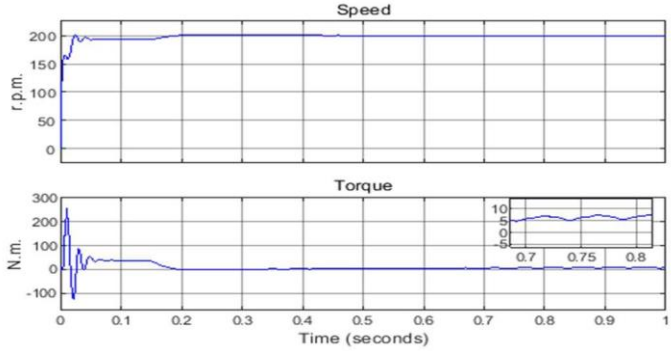

Figure 6. Speed and torque at direct starting of SERD

The speed reaches its steady state value within adequate time. The electric torque transient at starting is approximately 50 times its steady state magnitude (6 N.m.), as shown in Figure 6, which may cause damage to the machine even with its small duration.

3. Adding Parallel RL Impedance Between the Supply and the Stator Winding of the SERD

A 3-phase parallel R-L impedance is inserted between the supply and the stator windings, R=100 ohm and L= 0.1 H. The voltages, currents, and electric torque of the drive with such scheme are shown in figures 7-11 with reference speed equals 1.05 of the synchronous speed.

A considerable decrease in the magnitude of the starting stator current approximately twice its steady state value (± 5 amp.), is shown in Figure. 7, compared to its value without the added stator impedance, which reached 10 times its steady state value. The stator voltage is not affected.

The rotor voltage and current starting transient are presented in Figure. 8. The starting transient magnitude of the rotor voltage is high reaching 25 times its steady state value. It is worth noticing that the steady state magnitude of the rotor voltage slightly decreased than its rated value. A considerable decrease in the magnitude of the starting transient rotor current is observed. Its transient magnitude is only 5 times its steady state value, while it is 25 times its steady state value in the scheme without the stator impedance added. However, ripples are observed in the rotor voltage and current, decaying after 0.5 secs.

Consequently, a considerable decrease in the stator active and reactive power transients at starting are observed in Figure 9. There is still a high peak in the rotor active and reactive power due to the high transient of rotor voltage. However, these peaks' magnitudes are lower than its value without the added stator impedance. A large decrease in the starting magnitude of the DC voltage and current shown in Figure 10 compared to the case without the stator impedance. It is worth noticing that the rise in the DC voltage is gradual without starting peaks, in contrary with the SERD without added impedance. Also, its steady state magnitude is lower than the rated magnitude, following the decrease in the rotor AC voltage.

A decrease in the transient magnitude of the electric torque is clear in Figure. 11, about 5 times its steady state magnitude (5 N.m.), while a smooth rise in the rotor speed to its reference value is obtained.

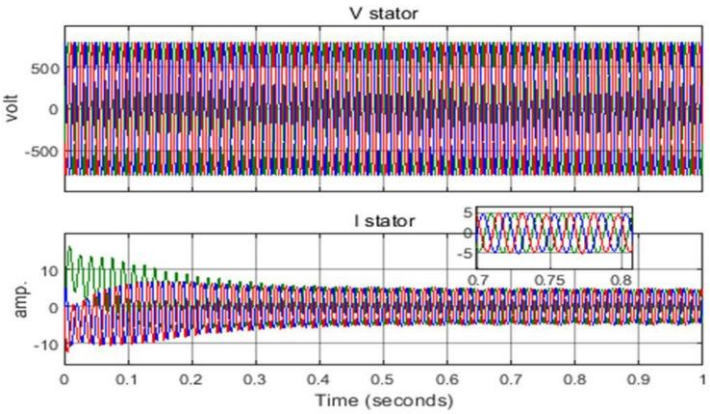

Figure 7. Stator voltage and current with added stator impedance

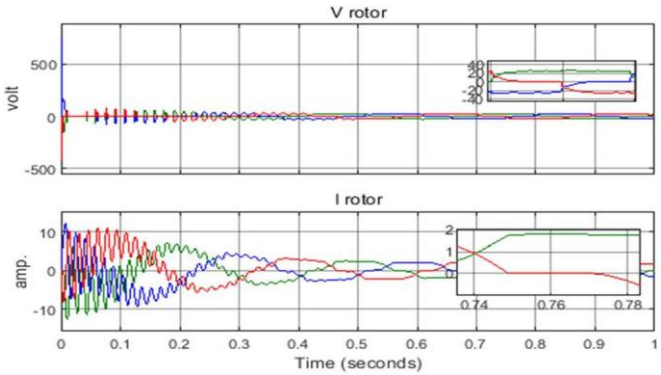

Figure 8. Stator voltage and current with added stator impedance

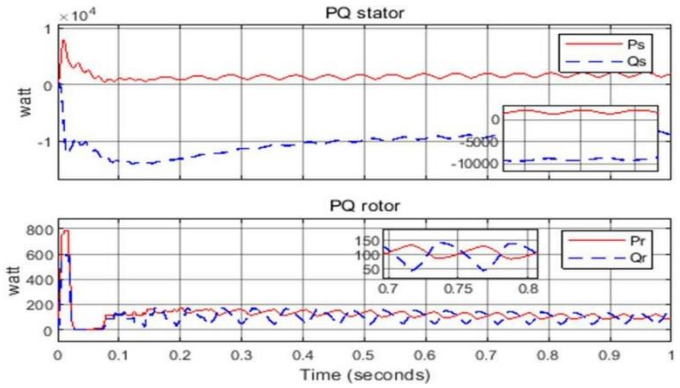

Figure 9. Stator and rotor active and reactive power with added stator impedance

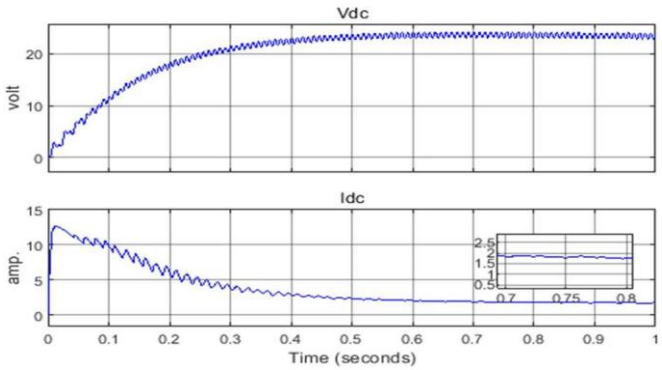

Figure 10. DC voltage and rotor current with added stator impedance

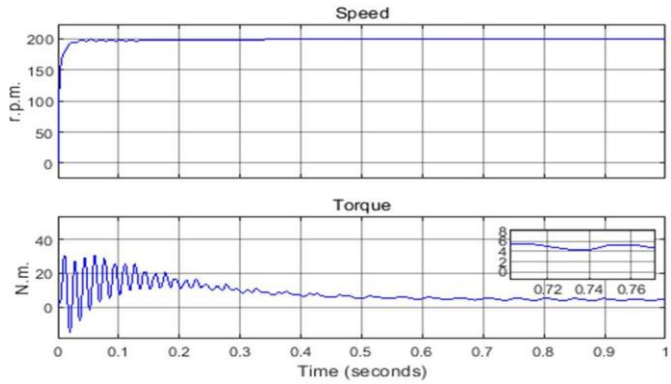

Figure 11. Speed and electric torque with added stator impedance

4. Adding Impedance in the Rotor Winding of the SERD

A 3-phase parallel R-L impedance is inserted between the rotor windings and the rectifier, R=100 ohm and L= 0.1 H The voltages, currents, and electric torque of the drive with such scheme are shown in figures 12-16 with reference speed equals 1.05 of the synchronous speed. A considerable decrease in the magnitude of the stator starting current is shown in Figure 12, compared to its value without any impedance. However, the transient current magnitude is higher than that in the case of added stator impedance, and its steady state value is also slightly higher due to the absence of limiting resistance. The stator voltage is not affected.

A decrease in the rotor voltage and rotor current starting transients is clear from Figure. 13. The steady state magnitude of the rotor current is higher than in the previous scheme (added stator impedance) due to the inductance of the added RL impedance. On the contrary, the steady state rotor voltage magnitude (about 30V) is lower than its value in the scheme of added stator impedance due to the loss in the resistance of the added rotor impedance the ripples observed in the rotor current fastly decayed compared to the scheme with added stator impedance.

The decrease in the stator active and reactive power starting transients are observed in Figure.14, with similar profile and approximate equal magnitudes as in the scheme added of stator impedance.

A large decrease in the DC voltage and current is shown in Figure 15 compared to the scheme without any impedance. The DC current transient profile is

similar to its profile with added stator impedance. However, the steady state DC voltage magnitude is lower, which is due to the effect of the added resistance.

A decrease in the transient torque magnitude is clear in Figure 16, with higher transient magnitude than when adding stator resistance. It is worth noticing that the steady state torque magnitude is higher than the rated value (7 N.m instead of 5 N.m.), due to the higher DC current. The speed profile is similar to the previous scheme.

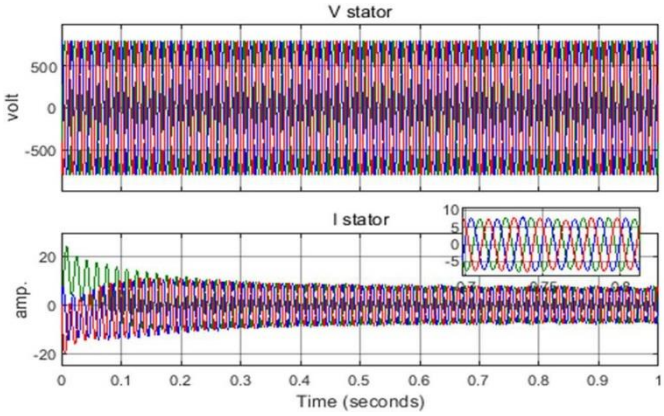

Figure 12. Stator voltage and current with added rotor impedance

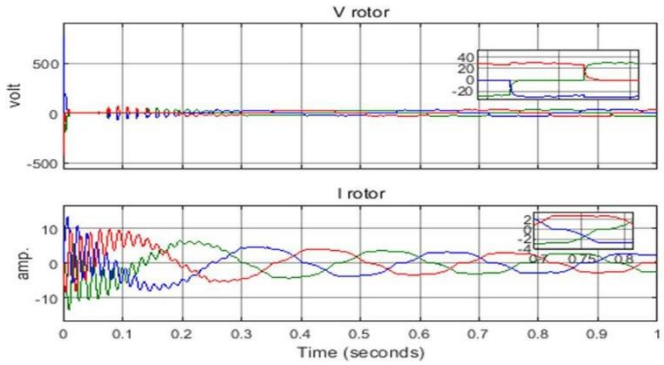

Figure 13. Rotor voltage and current with added rotor impedance

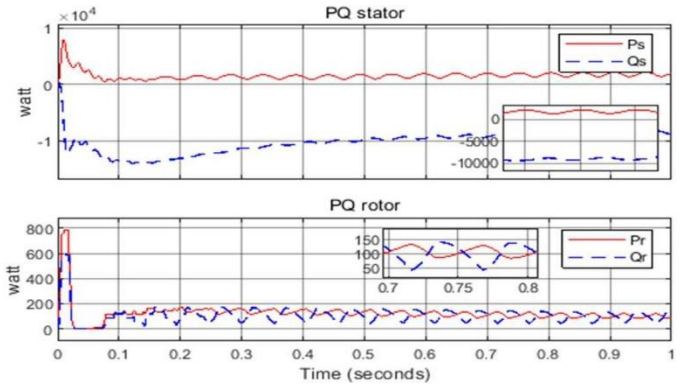

Figure 14. Stator and rotor active and reactive power with added rotor impedance

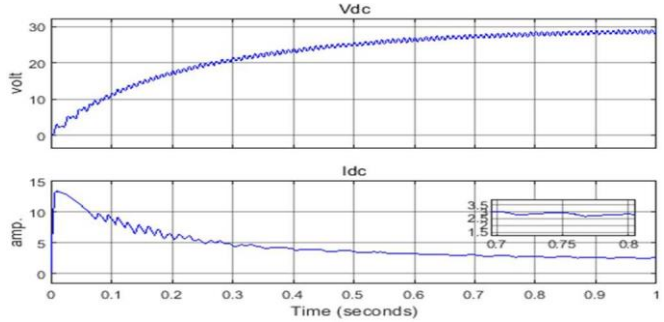

Figure 15. DC voltage and current with added rotor impedance

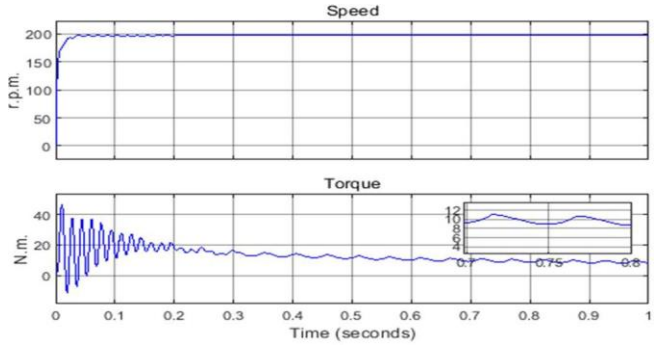

Figure16. Speed and electrical torque with added rotor impedance

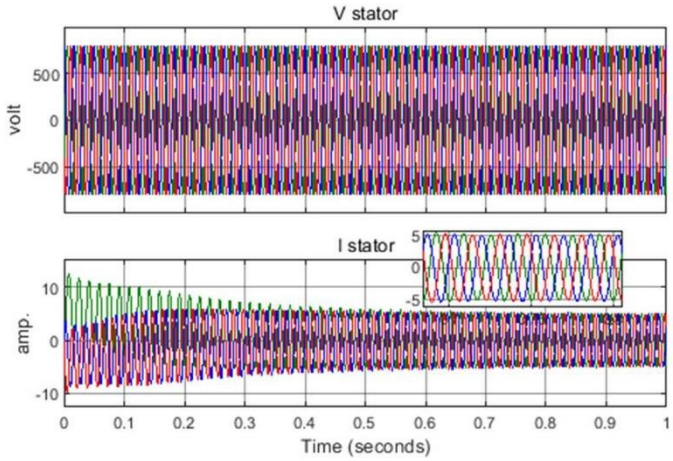

Figure 17. Stator voltage and current with both stator and rotor impedances

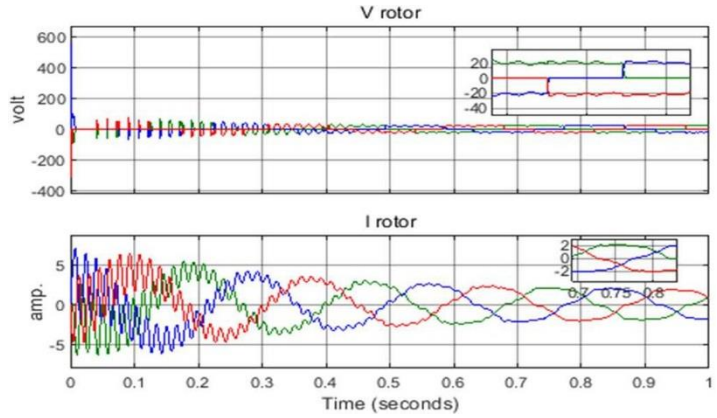

Figure 18. Rotor voltage and current with both stator and rotor impedances

5. Adding Impedances in the Stator and Rotor Windings of the SERD

Two 3-phase parallel R-L impedances are inserted, one between the supply and the stator windings, and the other one between the rotor windings and the rectifier, R=100 ohm and L= 0.1 H The voltages, currents, and electric torque of the drive with such scheme are shown in figures 17-21 with reference speed equals 1.05 of the synchronous speed.

The same considerable decrease in the magnitude of the starting current compared to the scheme without any impedance is shown in Figure 17. The same transient magnitude is observed as when adding stator impedance only. The steady state value of the stator current is achieved (5amp), after 0.3 second.

A decrease in the rotor voltage and rotor current starting transient is clear from Figure 18. It is worth noticing that the steady state magnitude of the rotor voltage is lower than the rated value (rated =25V, while with both impedances it equals 20V), due to losses in rotor added resistance. The ripples observed in the rotor current decayed after 0.7 secs., which is longer than its decay time in previous schemes.

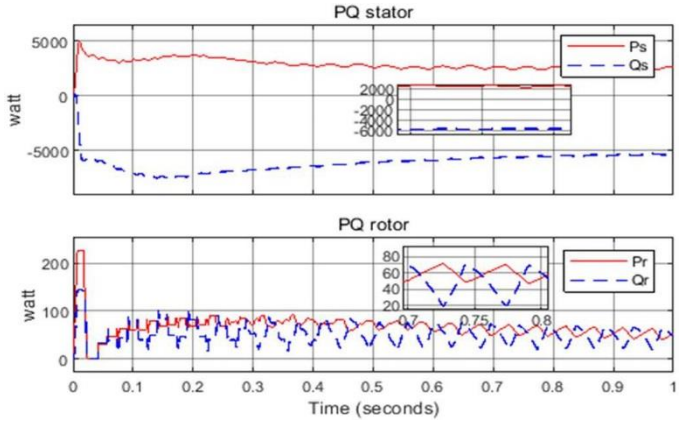

Figure 19. Stator and rotor active and reactive power with both stator and rotor impedances

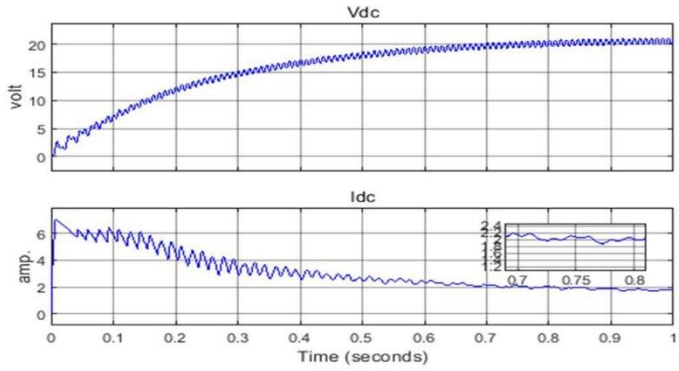

Figure 20. DC voltage and current with both stator and rotor impedances

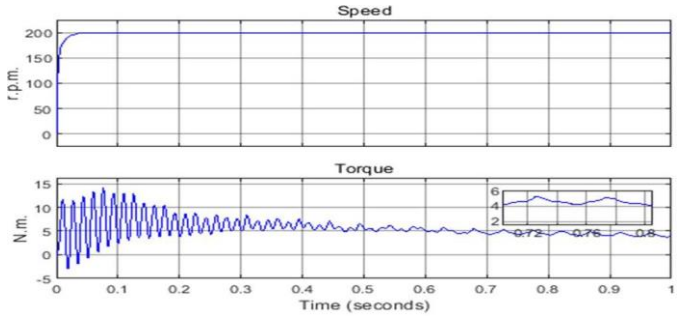

Figure 21. Speed and electrical torque with both stator and rotor impedances

The decrease in the starting transients of the stator active and reactive power shown in Figure 19 is similar to their decrease in the two previous schemes, i.e., that with stator added impedance and that with rotor added impedance. However, lower transient peaks are observed in the rotor active and reactive power than the two previous schemes. The considerable decrease in the DC current transient is clear in Figure 20 compared to the case without any impedance. The DC current transient is lower than in the two previous cases, i.e., that with stator added impedance and that with rotor added impedance. It is noted that, lower DC voltage than rated value, is obtained while the steady state DC current equals the rated value. However, the DC voltage contains the same ripples as in the two previous schemes without transient peaks. A decrease in the transient torque magnitude is clear in Figure 21, reaching its rated steady state magnitude after 0.4 sec, similar to its profile in the two previous schemes.

6. Conclusion

In this paper three schemes for damping stator and rotor voltages' and currents' starting transients in SERD are proposed. In the first scheme a parallel RL impedance is connected between the supply and the stator coils, in the second scheme a parallel RL impedance is added in the rotor circuit, and in the third scheme the two impedances are added simultaneously. Transient performance is simulated and the results of the three schemes are compared. Also, the effect of each proposed scheme on the steady state values of the SERD currents, voltages, and electric torque is studied and demonstrated.

Lower AC and DC currents' and voltages' transients, and consequently lower electric torque starting transient resulted when applying the proposed stator or rotor impedances. The steady state electric torque in the scheme with added rotor impedance is high than its rated value, which is not recommended. In both schemes, that with stator and that with rotor impedance, the peak transient of the rotor active and reactive power are still high. These transients are considerably decreased when adding both impedances simultaneously. It is worth noticing that in such scheme, the rotor power that is fed back to the supply is lower than its value in the other two schemes. This leads to decrease slightly the efficiency of the SERD. Hence it is concluded that the optimum scheme concerning the transients and steady state performance is when adding the both impedances.

References

[1] S. Ram, O.P. Rahi, V. Sharma, A comprehensive literature review on slip power recovery drives, Renewable and Sustainable Energy Reviews, 73 (2017) 922-934. [DOI]

[2] O.S. Ejiofor, O. Chinweike, I. Hillary, O. Titus, C.O. Ebele-Muolokwu, Dynamics of a Slip Power Recovery Scheme, Journal of Controller and converters, 4 (2019) 35-42. [DOI]

[3] I. Bhardwaj, B. Singh, Simulation and Comparative Assessment of Slip Power Recovery Scheme, International Journal of Advanced Research in Electrical, Electronics and Instrumentation Engineering, 6 (2017) 5294-5302.

[4] D. Muralidharan, P. Anitha Rani, R. Aswani, Efficiency Improvement of WRIM Using DSP Controller By Adding Rotor Capacitance, International Journal of Engineering Research & Technology (IJERT), 1 (2012) 1-10.

[5] S. Kumar, A. Kumar, H. Gupta, Comprehensive Analysis of Slip Power Recovery Scheme, International Journal of Innovative Research in Technology, 2 (2015) 28-33.

[6] E. Akpinar, P. Pillay MIEEE, K Ersak, Starting Transients in Slip Energy Recovery Induction Motor Drives- Part 2: Flowchart and Performance, IEEE Transactions on Energy Conversion, 7 (1992) 245-251. [DOI]

[7] W. Gu, J. Chu, and S. Gan, (2006) Starting performance research of a high-power middle-voltage induction motor soft starter based on the on-off transformer in 2006 IEEE International Symposium on Industrial Electronics, IEEE, (2006) 2063-2068. [DOI]

[8] S. Masoudi, M. Amirfakhrian, M. F. Abhari, A. Branch, A novel approach in soft starting of large induction motors, Australian Journal of Basic and Applied Sciences, 5 (2011) 296-299,

[9] J. Song-Manguelle, J. M. Nyobe-Yome, G. Ekemb, Pulsating torques in PWM multi-megawatt drives for torsional analysis of large shafts, IEEE Transactions on Industry Applications, 46 (2010) 130-138. [DOI]

[10] C.C. Yeh, N. A. O. Demerdash, Fault-tolerant soft starter control of induction motors with reduced transient torque pulsations, IEEE Transactions on Energy Conversion, 24 (2009) 848-859. [DOI]

[11] G. Zenginobuz, I. Cadirci, M. Ermis, C. Barlak, Performance optimization of induction motors during voltage-controlled soft starting, IEEE Transactions on Energy Conversion, 19 (2004) 278-288. [DOI]

[12] G. Zenginobouz, I. Cadrici, M. Ermis, C. Barlak, Soft starting of large induction motors at constant current with minimized starting torque pulsations, IEEE Transactions on Industry Applications, 37 (2001) 1334-1347. [DOI]

[13] P. Aree, Transient Torque Peak Reduction During DOL Starting of Three-Phase Induction Motors Using Zero-Crossing Switching Approach, IEEE Transactions on Energy Conversion, 36 (2021) 649-657. [DOI]

[14] Dwaraka S. Padimiti, Michael B. Christian, Jukka Jarvinen, Effective Transient-Free Capacitor Switching (TFCS) for Large Motor Starting on MV Systems, IEEE Transactions on Industry Applications, 55 (2019) 1012- 1020. [DOI]

[15] A. Aljabrine, H. Lei, H. Hess, B.K. Johnson, J. Geng, Superconducting Fault Current Limiter Application for Induction Motor Starting Current Reduction, IEEE Transactions on Applied Superconductivity, 29 (2019) 1-4. [DOI]

[16] Y. Xia, Y. Xu, M. Ai, J. Liu, Temperature Calculation of an Induction Motor in the Starting Process, IEEE Transactions on Applied Superconductivity, 29 (2019) 1-4. [DOI]

[17] Y. Xia, Y. Han, Y. Xu, M. Ai, Analyzing Temperature Rise and Fluid Flow of High-Power-Density and High-Voltage Induction Motor in the Starting Process, IEEE Acess, 7 (2019) 35588- 35595. [DOI]

[18] H. Sekhavatmanesh, J. Rodrigues, C.L. Moreira, J.A.P. Lopes, R. Cherkaoui, Optimal Load Restoration in Active Distribution Networks Complying with Starting Transients of Induction

Motors, IEEE Transactions on Smart Grid, 11 (2020) 3957- 3969. [DOI]

[19] S. Hasan, A.R. Nair, R. Bhattarai, S. Kamalasadan, K.M. Muttaqi, A Coordinated Optimal Feedback Control of Distributed Generators for Mitigation of Motor Starting Voltage Sags in Distribution Networks, IEEE Transactions on Industry Applications, 56, (2020) 864- 875. [DOI]

[20] S. Hasan, N. Gurung, K. M. Muttaqi, S. Kamalasadan, Electromagnetic Field-Based Control of Distributed Generator Units to Applied Superconductivity, 29 (2019) 1-4. [DOI]

[21] A. Damjanovic, Protection of Medium Voltage SCR Driven Soft-Starter from High-Frequency Switching Transients, IEEE Transactions on Industry Applications, 52 (2016) 4652- 4655. [DOI]

[22] Y. Park, H. Choi, J. Shin, J. Park, S.B. Lee, H. Jo, Airgap Flux Based Detection and Classification of Induction Motor Rotor and Load Defects During the Starting Transient, IEEE Transactions on Industrial Electronics, 67 92020) 10075- 10084. [DOI]

Conflict of interest

The Authors have no conflicts of interest to declare that they are relevant to the content of this article.

Does this article screened for similarity?

Yes

About the License